

Enhanced Nitrogen Removal and Distribution Distributions of Microbial Genes Associated with Nitrogen Cycling in A Vertical-flow Biofilter Treating Domestic Wastewater

Honglei Wang¹, Duntao Shu², Na Deng¹, Gehong Wei^{2*}, and Tongshun Wang³

¹State Key Laboratory of Soil Erosion and Dry Land Farming on the Loess Plateau, Institute of Soil and Water Conservation, Northwest A & F University, Yangling 712100, Shaanxi, China

²State Key Laboratory of Crop Stress Biology in Arid Areas, College of Life Sciences, Northwest A&F University, Yangling, Shaanxi 712100, China

³Jiangsu Hydraulic Research Institute, Nanjing 210029, Jiangsu, China

Research Article

Received date: 24/08/2018

Accepted date: 12/09/2018

Published date: 19/09/2018

*For Correspondence:

Honglei Wang, State Key Laboratory of Crop Stress Biology in Arid Areas, College of Life Sciences, Northwest A&F University, Yangling, Shaanxi 712100, China, Fax: +86 29 87091175, +86 29 87091175;

E-mail: wanghonglei@nwsuaf.edu.cn

Keywords: Domestic wastewater; Vertical-flow biofilter; Functional gene; Distribution contribution; Nitrogen removal.

Abbreviations: PCR: Polymerase chain reaction; APHA: American public health association; TP: Total phosphorous; TN: Total nitrogen; COD: Chemical oxygen demand

ABSTRACT

Vertical-flow biofilters have been investigated as a sustainable technology for nitrogen (N) and chemical oxygen demand (COD) removal from domestic wastewater. However, the distribution contributions of microbial genes responsible for removing N remain largely unexplored, particularly along the depth gradient in vertical-flow biofilters. Here, a three-stage vertical-flow bio-filter (three stages: P₁, P₂, and P₃) achieved large removal efficiencies for total nitrogen (TN; 87.00% and 33.69 g/m²-d), NH₄⁺-N (95.90% and 24.17 g/m²-d) and COD (92.00% and 558.15 g/m²-d). The removal contributions of NH₄⁺-N and TN in P₁, P₂, and P₃ can be ranked as follows: P₁ (45.9% and 38.4%, respectively) > P₂ (39.6% and 28.2%, respectively) > P₃ (10.6% and 20.5% respectively). The results revealed that *amoA*/bacteria, (*nirK* + *nirS* + *nosZ*)/bacteria, *amoA*/anammox and anammox/bacteria were the predominant gene groups responsible for NH₄⁺-N and TN removal in P₁, P₂ and P₃ and the contributions of these gene groups along the depth gradient of the bio-filter. Specifically, the NO₃⁻-N removal rate in P₃ was notably enhanced and collectively governed by the (*napA* + *narG*) and *nxrA* gene groups. Integrated analyses confirmed that the coupling of nitrification and denitrification governed the enhanced removal of NH₄⁺-N and TN in P₁. Combining anammox and nitrification contributed to the removal of NH₄⁺-N and TN in P₂. Enhanced anammox and denitrification accounted for the robust TN reduction in P₃. This study indicated that biofilters have great potential applicability for treating domestic wastewater without a sequential chain of treatments and extra aerations.

INTRODUCTION

Biofilter systems have been designed and deeply investigated as a widely applied technology for wastewater treatment [1-3]. Given their technological, economic and ecological superiority, biofilter systems are extensively constructed and adopted for N removal from domestic wastewater, especially in developing countries [4-7]. Nevertheless, numerous active biofilter systems show attenuated and limited reductions in TN levels [4-8]. Thus, the enhanced performance of TN treatment in biofilter systems is a critical task. In addition, increasing pollution discharges in rural villages across large areas in developing countries and stricter N discharge limitations ultimately prompt urgent efforts toward ameliorated engineering designs and the application of biofilter systems.

In a biofilter, wastewater traverses multilayer devices packed with various media (i.e., lava rocks, volcanic rocks, bioceramics, natural zeolites, gravel, and polyurethane foam), and air is immediately brought into the system [2,9]. However, microorganisms immobilized in the media degrade the COD and N through several pathways, such as nitrification, denitrification, and anammox [10-13]. It is generally accepted that biofilter systems can provide suitable aerobic areas for nitrification but generally lack sufficient anaerobic areas for anaerobic microorganisms (i.e., anammox and denitrification) to function well, which leads to nitrate ($\text{NO}_3\text{-N}$) accumulation and attenuated TN removal [5]. Previous studies have reported that single-stage biofilter systems are unable to efficiently remove TN because of their inability to synchronously provide suitable aerobic and anaerobic areas for both nitrifiers and denitrifiers [14]. Therefore, hybrid biofilter systems have been used to handle the continuous need for TN removal [5,8,15]. A denitrification biofilter was used [16] which was packed with reticulated polyurethane foam as a biofilm carrier for treating low carbon: nitrogen ratios (0.65–3.0) in wastewater and the TN removal efficiency ranged from 18.5 to 92.2%. A novel self-sustainable biofilm reactor was designed [4] with $\text{NH}_4\text{-N}$ and TN removal efficiencies of 94% and 79% ($9.84 \text{ g/m}^2\cdot\text{d}$), respectively. Average $\text{NH}_4\text{-N}$ and TN removal efficiencies of 69.3% (approximately $2.9 \text{ g/m}^2\cdot\text{d}$) and 54% (approximately $2.2 \text{ g/m}^2\cdot\text{d}$) was achieved respectively [17] in a sponge-bed trickling filter. The above results indicate that achieving high and stable TN removals in biofilters remains a challenge because of the various feedbacks of microorganisms associated with N cycling to different operating parameters and ambient conditions.

Vertical-flow biofilters have been devised as a simple and useful modification to strengthen the removal of COD, $\text{NH}_4\text{-N}$, and TN [18,19]. These biofilters generate a rhythmic sequential cycle of aerobic zones, aerobic-anaerobic zones and anaerobic zones, which enhances nitrification and denitrification in a single reactor. However, due to the different responses of N microorganisms to aerobic and anaerobic environments, microbial communities show large heterogeneities along the depth gradient in multiple treatment units in biofilters [20]. Previous studies have revealed that the aerobic environment in biofilter systems has a negative effect on denitrifying microorganisms to function well, and the carbon substances for denitrifying microorganisms are often deficient, as the carbon sources are available degraded which results in high $\text{NO}_3\text{-N}$ accumulation in the vertical-flow biofilters [21]. Thus, denitrification can be hypothesized as a rate-limiting TN removal process in vertical-flow biofilters. The co-occurrence of partial nitrification, denitrification, and anammox in bioreactors is known as a key factor responsible for the enhanced removal of $\text{NH}_4\text{-N}$ and TN [22,23]. Although the effects of vertical-flow biofilters on COD and $\text{NH}_4\text{-N}$ removal are largely explored, no further efforts have been made to enhance TN removal and investigate the underlying mechanisms of eliminating $\text{NO}_3\text{-N}$ accumulation and increasing TN removal, and the quantitative contribution of nitrogen to microbial genes in different treatment units in vertical-flow biofilters is still lacking. All of these unrevealed relationships limit our ability to improve the ability of TN removal.

In this study, we explore the feasibility of vertical-flow biofilters removing $\text{NH}_4\text{-N}$ and TN under various organic loads and the quantitative contribution of N microbes to TN removal. The main objectives are to evaluate the removal efficiencies of COD, $\text{NH}_4\text{-N}$ and TN in different treatment units in vertical-flow biofilters; to determine the predominant functional genes that shape $\text{NH}_4\text{-N}$ and TN removal in different treatment units and to quantify the distributional contributions of predominant functional genes in different treatment units (along the depth gradient).

MATERIAL AND METHODS

Experimental

Vertical-flow biofilter: A vertical-flow biofilter, with a working volume of 72 L, was built (Supporting Information, Figure S1). The biofilter was subdivided into three parts (P1, P2, and P3). P1 (with natural ventilation) consisted of two functional layers (for each layer, $L \times W \times H = 20 \times 20 \times 30 \text{ cm}^3$) which were filled with lava rocks (particle size: 5-8 mm) and bioceramics (particle size: 5-8 mm). P2 (with natural ventilation) consisted of two functional layers (for each layer, $L \times W \times H = 20 \times 20 \times 30 \text{ cm}^3$) which were packed with lava rocks (particle size: 2-5 mm) and bio-ceramics (particle size: 2-5 mm). P3 (without ventilation) consisted of one functional layer ($L \times W \times H = 20 \times 20 \times 60 \text{ cm}^3$) which was packed with polyurethane foaming plastic with 1 to 2 mm apertures. A bistratal sieve tray (thickness: 2 cm) was installed between the treatment layers of P1 and P2 to mix wastewater and air.

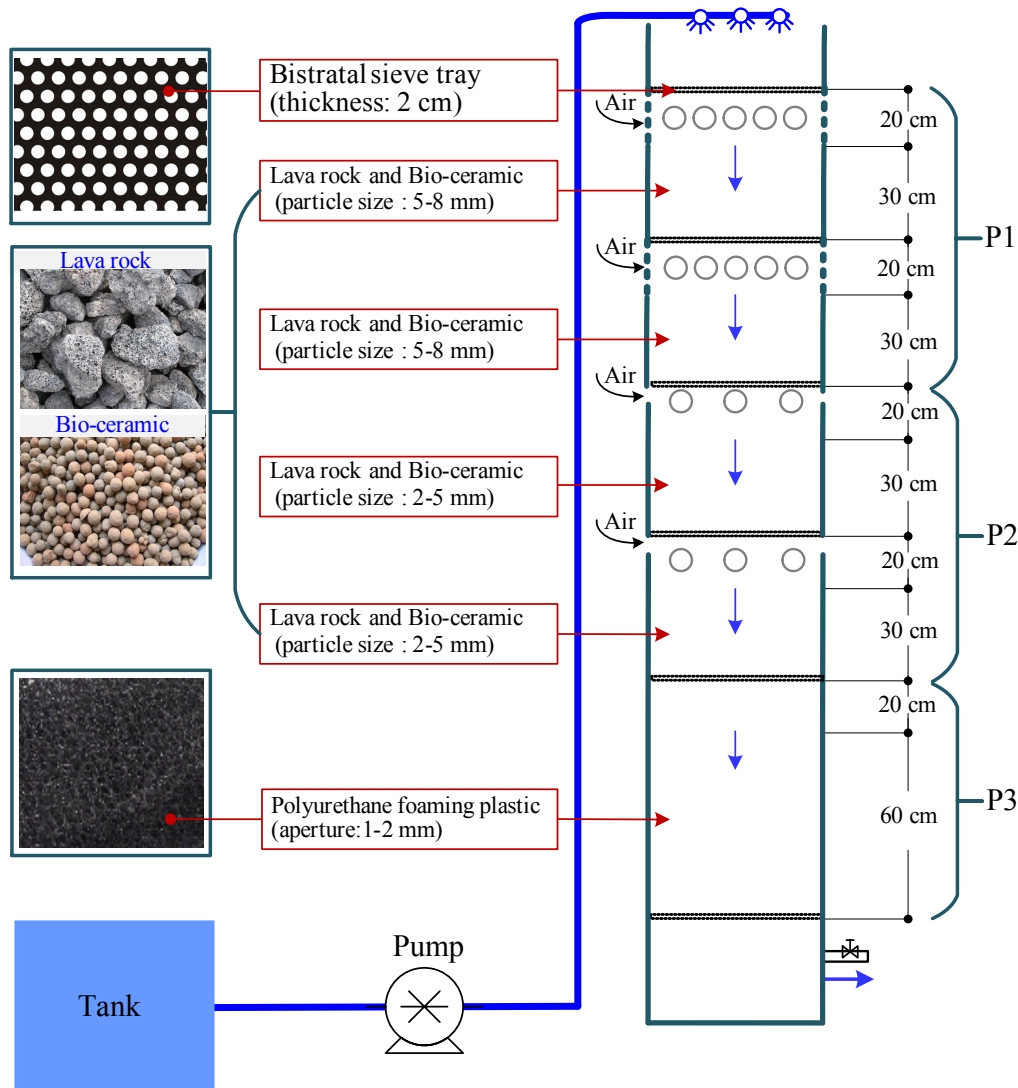


Figure S1: Schematic diagram of the vertical-flow biofilter

According to our actual environmental quality surveys, the average COD and NH₄⁺-N concentrations in domestic wastewaters were 342.65 ± 86.52 mg/L and 28.30 ± 12.25 mg/L respectively. The synthetic wastewater was made from tap water (NO₃⁻-N: 4.2-6.9 mg/L). In this study, the synthetic wastewater contained 200-600 mg/L of COD, 20-40 mg/L of NH₄⁺-N, 25.49-47.91 mg/L of TN and 3-4 mg/L of TP was fed into the vertical-flow biofilter. The hydraulic loading rate was 1.0 m³/m².d. The basic composition of the synthetic wastewater in each operation stage is organized in **Table 1**. The vertical-flow biofilter was installed indoors and the temperature and pH in the influents and effluents ranged from 18.5°C to 26.8°C and 7.2 to 8.1 respectively. The experiment included a start-up stage (five weeks) and operational stage (0-140 days) and the entire experiment lasted a total of 175 days.

Table 1: Synthetic wastewater composition in each stage.

| Parameters | Stage I | Stage II | Stage III | Stage IV | Stage V |
|--|---------|----------|-----------|----------|---------|
| COD (C ₆ H ₁₂ O ₆ , mg/L) | 200 | 300 | 400 | 500 | 600 |
| NH ₄ ⁺ -N (NH ₄ Cl, mg/L) | 20 | 25 | 30 | 35 | 40 |
| C/N ratio | 10.00 | 12.00 | 13.33 | 14.29 | 15.00 |
| TP (KH ₂ PO ₄ , mg/L) | 3.0 | 3.2 | 3.5 | 3.8 | 4.0 |
| Time (day) | 0~28 | 29~56 | 57~84 | 85~112 | 113~140 |

All the chemical reagents used in this study were of Analytical Reagent (AR) grade.

Samples

Water samples were extracted from P₁, P₂, and P₃ one time each week. The water quality indexes (i.e. COD, NH₄⁺-N, nitrite (NO₂⁻-N), NO₃⁻-N, TN, DO, and pH) of the influents and effluents were measured using standard techniques, and standard analytical procedures for the variables are described elsewhere [22-24]. The microbial samples (both lava rock/bioceramic and polyurethane foaming plastic) were collected from the biofilter at the end of days 14, 28, 42, 56, 70, 84, 98, 112, 126, and 140. At every sampling time, five microorganism samples were gathered from P₁, P₂, and P₃. Then, the samples were stored in a -20°C ice incubator and ready for DNA extraction. The OMEGA soil extraction kit (D5625-01) was used to extract genomic DNA from the samples (e.g. from the 0.5 g to 1.0 g sample) [23]. Then, the genomic DNA was stored in a -20°C ice incubator.

Quantitative PCR

The *amoA* and anammox genes are currently known as the markers of aerobic ammonia oxidation and anoxic ammonia oxidation, respectively [25,26]. The *nxrA* gene is currently known as the marker of NO₂⁻-N oxidation [30]. The periplasmic nitrate reductase (*napA*, NO₃⁻-N → NO₂⁻-N), membrane-bound nitrate reductase (*narG*, NO₃⁻-N → NO₂⁻-N), nitrite reductase (*nirK/nirS*, NO₂⁻-N → NO), and nitrous oxide reductase (*nosZ*, N₂O → N₂) are widely adopted as markers for denitrifying bacteria. A PCR was performed with primer pairs Eub338f/Eub518r for total bacteria [27], Ar109f/Ar344r for *archaea* [28], Amx809f/Amx1066r for *anammox* [29], amo598f/amo718r for *amoA* [26], F1norA/R1norA for *nxrA* [30], V17F/4R for *napA* [31], 1960 m2f/2050 m2r for *narG* [32], 583F/909R for *nirK* [33], nirScd3aF/nirSR3cd for *nirS* and 1527F/1773R for *nosZ* [34]. The qPCR was adopted to quantify the population dynamics of N microbial genes in the biofilter (P₁, P₂, and P₃) with a 20 μL reaction mixture [16,35]. The detailed protocol and parameters for each marker are described elsewhere [16,23].

Data Processing and Statistics

Influent and effluent concentrations were adopted to quantify the removal efficiencies (%). Influent and effluent concentrations, hydraulic retention times (2.0 h) and the working volumes of functional layers (V = 0.2 × 0.2 m²) were collectively adopted to quantify the removal rates of NH₄⁺-N, NO₃⁻-N and TN (g/m².d). Standard deviations (SDs) in the population dynamics of the N microbial genes were analyzed using three duplicated data via the qPCR. The population dynamics of the N microbial genes and other ratios of the N microbial genes (e.g. *amoA*/bacteria, (*nirK* + *nirS* + *nosZ*)/bacteria and *nxrA*/bacteria) were adopted as candidate-independent variables in the linear regression analysis, with SPSS 20 to link with the N removal rates (i.e. NH₄⁺-N, NO₃⁻-N and TN). A pathway analysis was adopted to quantify the contributions of key functional genes (i.e. functional gene groups) to the N removal rates.

RESULTS AND DISCUSSION

Treatment Performance of the Biofilter

During the operation, the vertical-flow biofilter achieved high COD removal efficiencies (92.15 ± 2.91%) (Figure 1a). P₁, P₂, and P₃ accounted for 30.50 ± 9.20%, 44.22 ± 12.57% and 17.43 ± 6.79% of COD removal respectively (Figure 1b). It is hypothesized that the removal efficiencies of the COD are higher than those in other biofilter systems based on traditional methods and newly discovered methods with artificial aerations, which are currently used to treat domestic wastewater (COD=120–450 mg/L) with gross COD removal efficiencies fluctuating from 50% to 89% [7,36,37]. The average rates for COD transformation in P₁, P₂, and P₃ were 174.14 ± 66.69 g/m².d, 288.76 ± 163.78 g/m².d and 95.26 ± 37.36 g/m².d respectively. The biofilter achieved a COD removal rate of 558.15 ± 208.47 g/m².d (Figure S2), which was higher than the treatment performances of CODs investigated in previous studies (e.g. 437.00 g/m².d by [38] and 275.25 g/m².d by [5]). The above results revealed the COD removal contributions of P₁, P₂, and P₃ along the depth gradient (from top to bottom). This high COD removal performance was due to the sieve tray operation in P₁ (with natural ventilation) and P₂ (with natural ventilation) which allowed for wastewater/air contact. However, P₃ (without ventilation, Figure S1) achieved a lower COD removal compared with P₁ and P₂. This was because most denitrifiers are heterotrophic bacteria which utilize organic C as a required organic source; this leads to the continued consumption and loss of COD [16,39].

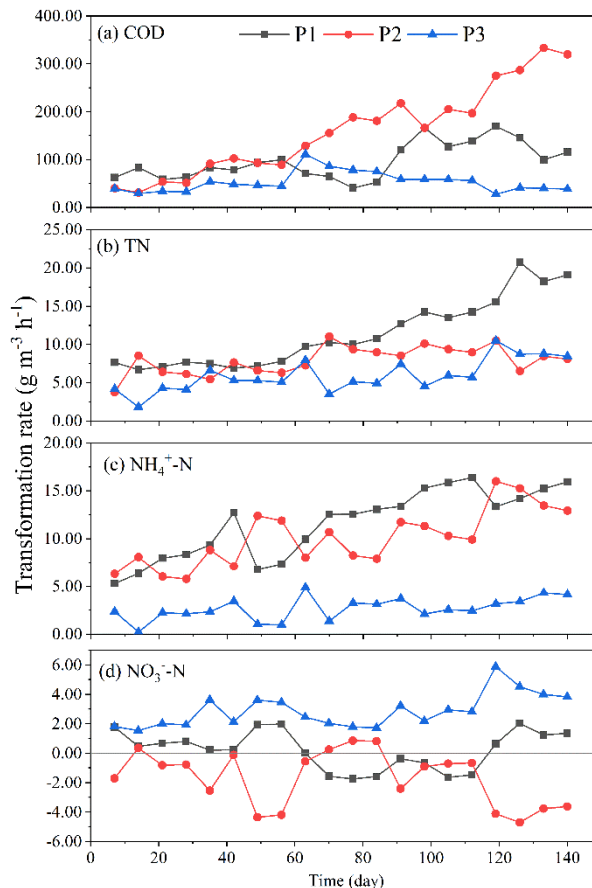


Figure S2: Long-term dynamic transformation rates of nitrogen in the biofilter

It is well known that vertical-flow biofilters can effectively remove COD and $\text{NH}_4\text{-N}$ [8,38,40]. Here, we focus our discussion on the TN removal and effluent which was identified as an indicator for the simultaneous monitoring of multiple water treatment performances. As the COD increased from 200 mg/L to 600 mg/L, the $\text{NH}_4\text{-N}$ removal efficiency stabilized at $95.88 \pm 2.45\%$ (**Figure 1c**). The biofilter achieved a TN removal efficiency of $87.28 \pm 4.12\%$. According to previous study [5,41], it has been reported that a TN85.4% using a vertical-flow biofilter when integrated with a horizontal-flow multisoil-layering reactor. In other hybrid biofilters, TN removal efficiencies range from 66.5% to 83% [37,42]. In this study, the biofilter achieved even higher TN removal efficiency (maximum of $46.5 \text{ g/m}^2\text{-d}$). TN removal rates of $27.83\text{-}30.62 \text{ g/m}^2\text{-d}$ in a vertical-flow biofilter and horizontal-flow multisoil-layering reactor was reported [5]. TN removal rates in hybrid biofilters of 2.34 and $9.84 \text{ g/m}^2\text{-d}$ was achieved respectively [4,17]. An average TN removal rate of $0.11 \text{ kg/m}^3\text{-d}$ (approximately $0.86 \text{ g/m}^2\text{-d}$) in a partial nitrification-anammox biofilter was reported [7]. The high and stabilized removals of $\text{NH}_4\text{-N}$ and TN in the biofilter were comparable with the values reported in the vertical-flow biofilters used for treating rural wastewater [5], multimedia biofilters used for treating for sewage treatment [20], simultaneous nitrification-denitrification biofilters [43] and anammox biofilm reactors used for the removal of nitrogen from wastewater [4,7]. In addition, the average TN effluent concentrations ($4.23 \pm 0.5 \text{ mg/L}$) were lower than those in aerobic or anaerobic biofilter systems, with a practical effluent concentration fluctuating from 5.17 mg/L to 13.1 mg/L [7,44,45].

The dynamic transformation of nitrogen in P_1 , P_2 , and P_3 is shown in **Figure 2** and **Figure S2**. P_1 , P_2 , and P_3 accounted for $45.93 \pm 7.70\%$, $39.56 \pm 9.39\%$, and $10.65 \pm 4.26\%$ of the $\text{NH}_4\text{-N}$ removal (**Figure 1d**) respectively. P_1 , P_2 , and P_3 accounted for $37.72 \pm 3.95\%$, $28.24 \pm 5.49\%$, and $20.32 \pm 4.73\%$ of the TN removal, respectively. The residual $\text{NH}_4\text{-N}$ in the effluent markedly decreased from 16.09 mg/L (P_1) to 1.00 mg/L (P_3). This distinct decline in the $\text{NH}_4\text{-N}$ effluent was attributed to the natural ventilation in P_1 and P_2 (**Figure S1**), leading to the enhanced nitrification responsible for eliminating the accumulation of $\text{NH}_4\text{-N}$ and $\text{NO}_3\text{-N}$ in the system (**Figure 2** and **Figure S2**). Together, these results are consistent with those in previous studies, suggesting that biofilter systems with aeration operations enable the effective removal of COD and $\text{NH}_4\text{-N}$ and contribute to residual $\text{NO}_3\text{-N}$ and TN in the effluent [7,21,42]. Throughout this study, apparent declines in the $\text{NO}_3\text{-N}$ and TN effluent concentrations in P_3 (without air supply, **Figure S1**) are observed in **Figure 2c**, indicating that denitrification was sufficient for $\text{NO}_3\text{-N}$ and TN removal. P_3 had a significantly higher rate of $\text{NO}_3\text{-N}$ transformation ($3.83 \text{ g/m}^2\text{-d}$) than those in P_1 ($0.29 \text{ g/m}^2\text{-d}$) and P_2 ($-2.24 \text{ g/m}^2\text{-d}$), suggesting that the

functional layer without an oxygen supply plays an important role in enhancing the denitrification process to achieve effective NO₃--N and TN removal.

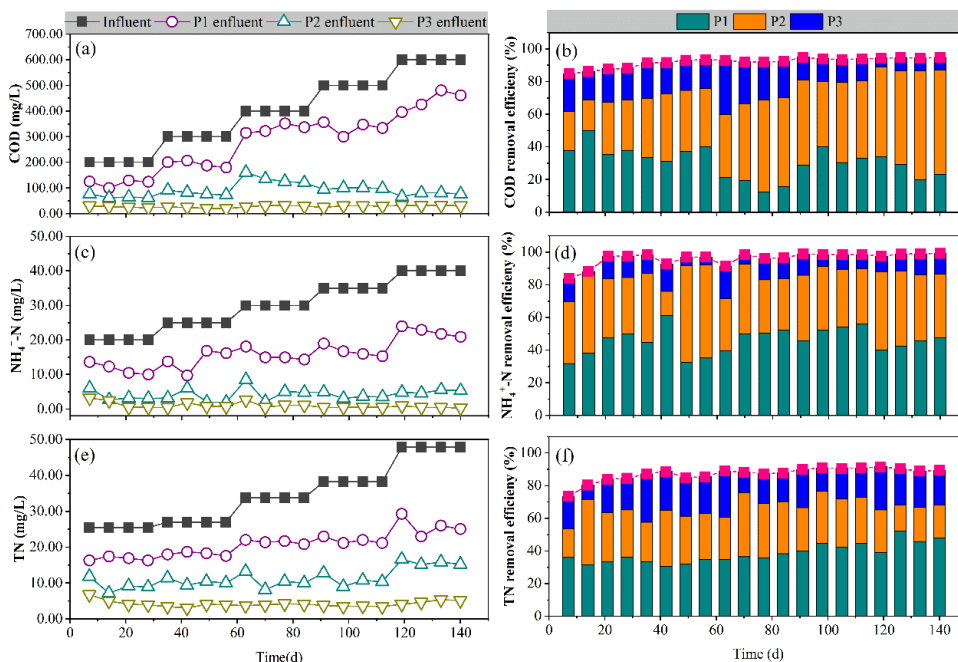


Figure 1: Influent concentrations, effluent concentrations and removal efficiencies of COD (a, b), NH₄⁺-N (c, d), and TN (e, f) in the vertical-flow biofilter along the depth gradient.

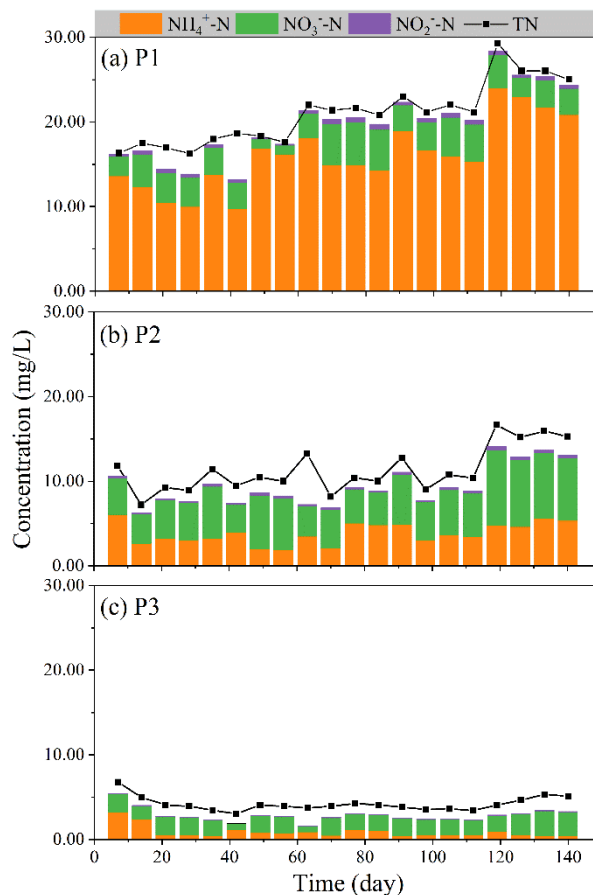


Figure 2: Long-term dynamic transformation of nitrogen in the vertical-flow biofilter along the depth gradient.

Nitrogen Removal Mechanisms

The experiment was divided into a startup stage (five weeks) and operational stage (0-140 days). The abundances of bacteria, archaea, and N microbial genes in P₁, P₂, and P₃ were quantified throughout the phases of operation to estimate the changes in their numbers, which reveals the evolution of N removal pathways in P₁, P₂, and P₃.

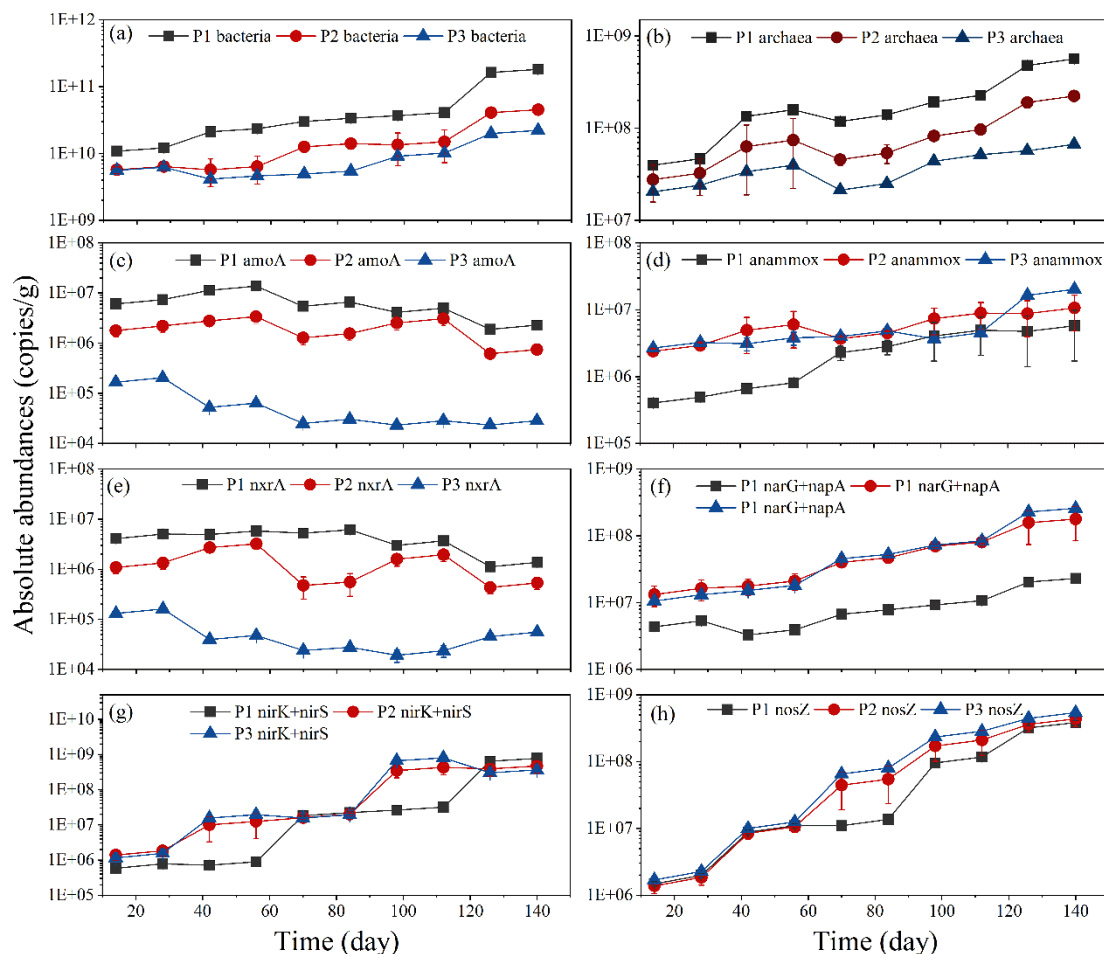


Figure 3: Dynamic populations of microbial communities and functional genes in the vertical-flow biofilter along the depth gradient: bacteria (a), archaea (b), amoA (c), anammox (d), nxrA (e), narG + napA (f), nirK + nirS (g), and nosZ (h).

The results from **Figure 3a** indicate that the absolute abundances of bacteria in P₁, P₂, and P₃ showed rapid increases by 12.35, 7.21, and 3.54-fold respectively over the entire period. These increases directly enhanced the continuous consumption of COD, leading to 2.03, 7.16, and 1.07-fold increases in the COD removal efficiencies of P₁, P₂, and P₃ respectively. In this study, the COD concentrations increased from 200 mg/L to 600 mg/L, leading to an enhanced supplemental substrate for the bacteria community in the biofilter and causing rapid enrichment and growth [39]. The archaea in P₁, P₂, and P₃ increased from 2.75×10^7 copies/g on day 14 (operational stage) to 5.67×10^8 copies/g on day 140, exhibiting low abundance and similar patterns relative to the change in COD concentration. Although *archaea* revealed much smaller amounts compared to bacteria **Figure 3b**, the *archaea* community may play a key role in NH₄⁺-N removal [46,47].

The NH₄⁺ transformation communities harboring specific catabolic nitrifying-ammonium monooxygenase (*amoA*) and anaerobic ammonium-oxidizing (*anammox*) microorganisms are organized in **Figure 3c** and **Figure 3d** respectively. As the COD concentration increases, the abundance of *amoA* in P₁, P₂, and P₃, with overall declining trends and similar patterns, varied between 2.13×10^4 copies/g and 7.39×10^6 copies/g. However, the abundance of *anammox* in P₁, P₂ and P₃ with overall increasing trends and similar patterns, varied between 4.89×10^5 copies/g and 2.02×10^7 copies/g. The absolute abundance of *amoA* in P₁ on day 14 was 15.10 times greater than that of *anammox*. These results indicate that aerobic ammonia oxidation was the controlled NH₄⁺-N removal pathway (45.93% of NH₄⁺-N removal, **Figure 1d**). Meanwhile, the ratio of *amoA* to *anammox* in P₂ on day 14 was approximately 0.75, suggesting that the relationship between the nitrification and *anammox* processes was the predominant factor responsible for high NH₄⁺-N removal (39.56% of NH₄⁺-N removal, **Figure 1d**). The *anammox* in P₃ on day 7 was 16.02 times greater than *amoA*, indicating that anaerobic ammonia oxidation was a key NH₄⁺-N removal pathway (10.65% of NH₄⁺-N removal, **Figure 1d**). After 140 days

of operation, the ratios of *anammox* to *amoA* in P₁, P₂ and P₃ were approximately 0.39, 14.19 and 947.16 respectively, suggesting that nitrification in P₁ and anammox in P₂ and P₃ were dominant NH₄⁺-N removal pathways responsible for the robust NH₄⁺-N removal (96.14%, **Figure 1d**). The above findings suggest that the *anammox* process was observably enhanced and eventually superseded nitrification as the predominant NH₄⁺-N removal pathway in the vertical-flow biofilter. As the COD concentration increased, the DO was continuously consumed during the process of organic matter oxidation (92.15% of COD removal, **Figure 1b**), creating intensive microdomain anaerobic environmental conditions in P₁, P₂ and P₃, which were suitable for the growth of anaerobic oxidizing (*anammox*) bacteria as the governing driver of NH₄⁺-N removal [3,4,48].

During the entire period, the *nrxA* gene slightly showed decreases in P₁, P₂, and P₃, leading to attenuated nitrification activity, which accounted for the reduced production of NO₃⁻-N. Five denitrifying genes (i.e., *narG*, *napA*, *nirK*, *nirS*, and *nosZ*) are shown in **Figures 3f-3h**. All five genes showed increases in P₁, P₂, and P₃, resulting in increased denitrification that accounted for the NO₃⁻-N removal. The synchronous growth of these five genes in the biofilter was due to their similar adaptations to anoxic environments and their associated yet distinct ecological niches [31,49,50]. Previous studies have indicated that denitrification is the dominant pathway, and the rate-limiting process is attributed to achieving a high TN removal [8,23]. In this study, the abundances of the five genes in P₂ (with natural ventilation) and P₃ (without natural ventilation) were 1.40 and 1.81 times greater respectively, than those in P₁ (with natural ventilation), leading to higher contributions of P₂ and P₃ that were responsible for TN (48.56% of TN removal, **Figure 1f**) than those of P₁ (38.72% of TN removal, **Figure 1f**). This might also explain the corresponding high TN removal in the biofilter compared to that in other biofilters for wastewater treatment [5,16,51].

Nitrogen Transformation Pathway

Quantitative relationships were determined to connect macroscale NH₄⁺-N and TN removal and functional genes associate with the nitrogen cycle and improve the understanding of predominant functional genes that control the NH₄⁺-N and TN removal processes in P₁, P₂, and P₃. By introducing a number of specific variables into the linear stepwise regression models [23], the equations of NH₄⁺-N, NO₃⁻-N, and TN were built with R² > 0.819 (**Table 2**).

Table 2: Quantitative response relationships between the nitrogen transformation rates and functional gene groups in P₁, P₂, and P₃.

| Stepwise models | regression | Equations | R ² | P | F |
|-----------------|------------|---|----------------|-------|---------|
| P ₁ | | NH ₄ ⁺ -N = 54.793 <i>amoA</i> /bacteria + 41.906(<i>nirK</i> + <i>nirS</i> + <i>nosZ</i>)/bacteria - 80.831 | 0.966 | 0.034 | 28.803 |
| | | NO ₃ ⁻ -N = -6.387 <i>nrxA</i> /(<i>napA</i> + <i>narG</i>) - 4.258 <i>nrxA</i> /bacteria +9.955 | 0.993 | 0.007 | 135.545 |
| | | TN = 22.231(<i>nirK</i> + <i>nirS</i> + <i>nosZ</i>)/bacteria - 5.820 <i>nrxA</i> /(<i>napA</i> + <i>narG</i>) - 13.337 | 0.996 | 0.004 | 236.885 |
| P ₂ | | NH ₄ ⁺ -N = -66.063 <i>amoA</i> / <i>anammox</i> + 3.368 <i>nrxA</i> +50.874 | 0.995 | 0.005 | 211.103 |
| | | NO ₃ ⁻ -N = 8.531(<i>napA</i> + <i>narG</i>)/ <i>nrxA</i> - 9.724 | 0.819 | 0.035 | 13.599 |
| | | TN = -0.301 <i>amoA</i> / <i>anammox</i> + 17.674 <i>nosZ</i> /bacteria - 4.872 | 0.824 | 0.039 | 14.666 |
| P ₃ | | NH ₄ ⁺ -N = 5.097 <i>anammox</i> / <i>amoA</i> - 4.715 | 0.915 | 0.023 | 32.147 |
| | | NO ₃ ⁻ -N = 1.495 <i>anammox</i> / <i>amoA</i> + 1.417(<i>napA</i> + <i>narG</i>)/ <i>nrxA</i> - 1.956 | 0.980 | 0.020 | 49.974 |
| | | TN = 74.686 <i>anammox</i> /bacteria + 4.703(<i>napA</i> + <i>narG</i> + <i>nirK</i> + <i>nirS</i> + <i>nosZ</i>)/bacteria - 55.442 | 0.949 | 0.046 | 18.394 |

The results showed that the NH₄⁺-N reduction rate in P₁ was significantly correlated with the ratios of *amoA*/bacteria and (*nirK* + *nirS* + *nosZ*)/bacteria. A greater direct contribution of (*nirK* + *nirS* + *nosZ*)/bacteria (65.8%) to the NH₄⁺-N reduction compared with *amoA*/bacteria (30.8%) was observed in P₁ over the entire period **Figure 4a**. The first variable, *amoA*/bacteria, shows a level of NH₄⁺-N removed via the nitrification process (NH₄⁺-N → NO₂⁻-N), which results in positive relations with the NH₄⁺-N reduction rate, while the variable (*nirK* + *nirS* + *nosZ*)/bacteria was positively correlated with NH₄⁺-N removal. It is generally accepted that nitrification and denitrification are adverse processes that function well under aerobic and anaerobic environmental conditions respectively [52]. Our results indicated the functional

interplay between nitrifiers and denitrifiers which is in agreement with [53] who suggested that the polyphyletic distribution of denitrifying genes leads to their co-occurrence with nitrifying genes in many strains. The NO_3^- -N accumulation rate was negatively correlated with $nxrA/(napA + narG)$ and $nxrA/bacteria$ (Table 1). A greater direct contribution of $nxrA/(napA + narG)$ (-64.7%) to NO_3^- -N accumulation compared with $nxrA/bacteria$ (-33.8%) was observed in P1 (Figure S3a). The $nxrA$ gene is related to NO_3^- -N production, while the $napA$ and $narG$ genes are related to NO_3^- -N consumption. Thus, the ratios of $nxrA/(napA + narG)$ and $nxrA/bacteria$ are defined as the NO_3^- -N accumulation. The TN transformation in P₁, related to the nitrification and denitrification processes, was jointly controlled by $(nirK + nirS + nosZ)/bacteria$ and $nxrA/(napA + narG)$. A greater direct contribution of $(nirK + nirS + nosZ)/bacteria$ (90.9%) to TN reduction compared with $nxrA/(napA + narG)$ (-21.0%) was observed in P₁ over the entire period (Figure 4a). The above results indicate the close relationship between nitrification and denitrification processes was contributed to the robust NH_4^+ -N and TN removal performances in P₁ [36,54].

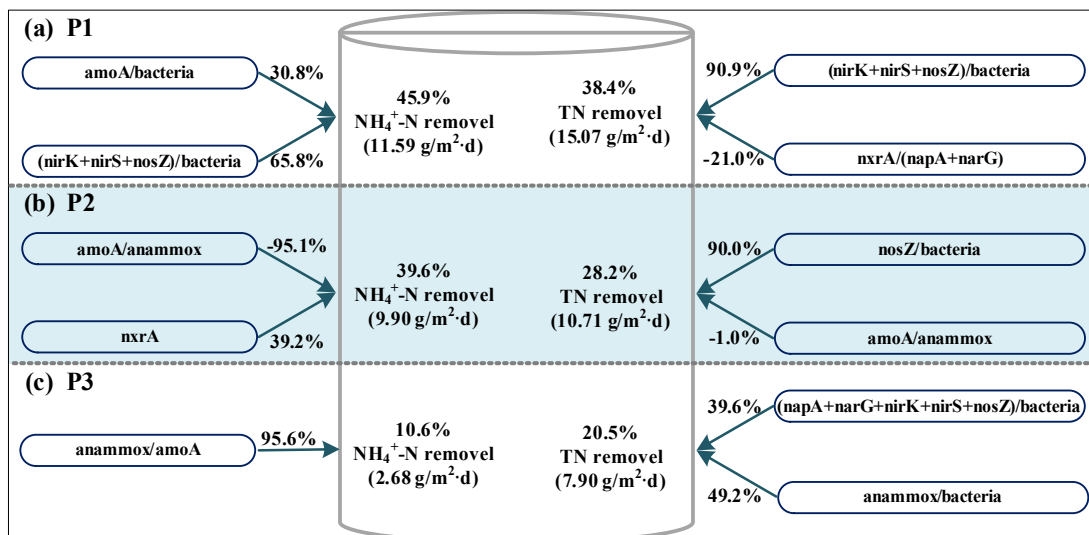


Figure 4: Pathway diagrams estimating the direct contributions of functional gene groups to NH_4^+ -N and TN removal in P₁, P₂, and P₃. The arrows designate the direction of causality. The numbers adjacent to the arrows represent the degree of the direct contributions, and the positive and negative numbers represent the positive and negative contributions respectively.

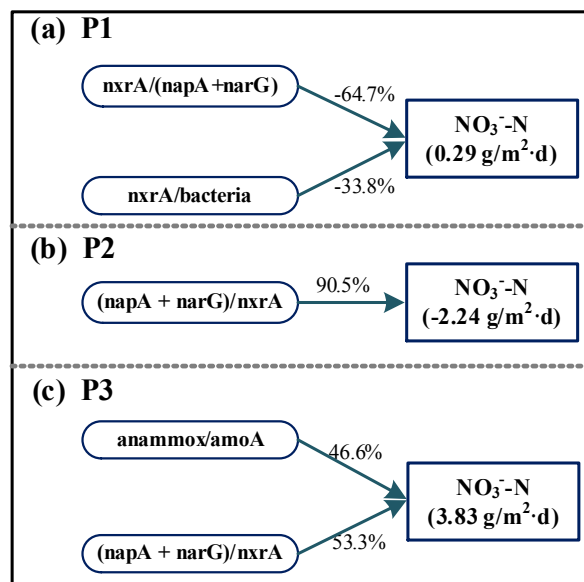


Figure S3: Pathway diagrams assessing the effects of functional gene groups on the NO_3^- -N transformation rate (or accumulation rates if the effluent NO_3^- -N concentration increased).

The NH_4^+ -N reduction rate in P₂ was negatively correlated with $amoA/anammox$. A greater direct contribution of $nxrA$ (39.2%) to the NH_4^+ -N reduction compared with $amoA/anammox$ (-95.1%) was observed in P₁ over the entire period (Figure 4a). This was because the ammonia-oxidizing bacteria (AOB) accounted for the production of NO_2^- -N (NH_4^+ -N \rightarrow NO_2^- -N), whereas $anammox$ was responsible for NO_2^- -N consumption. However, AOB associated with the NH_4^+ -N transformation are often restrained by the accumulation of NO_2^- -N [22,55,56]. The NO_2^- -N accumulation is known as the

ratio of *amoA/anammox*. This is because the *amoA* gene is linked with NO_2^- -N production (NH_4^+ -N \rightarrow NO_2^- -N), whereas *nrxA* and *anammox* are associated with the consumption of NO_2^- -N [39]. This result shows the ecological association between *nrxA* and *anammox* during the removal process of NH_4^+ -N, which is usually considered to be dominated and actuated by only the *amoA* gene. The NO_3^- -N transformation is governed by the ratio of $(\text{napA} + \text{narG})/\text{nrxA}$ because of the two homogenous function genes (*napA* and *narG*) linked with NO_3^- -N consumption, whereas nitrite oxidizing bacteria (*nrxA*) is responsible for NO_3^- -N production. The results from Figure S₃b indicate that $(\text{napA} + \text{narG})/\text{nrxA}$ was the predominant gene group contributing to high NO_3^- -N reduction (90.5%) in P₂. The TN reduction rate in P₂ was jointly controlled by *amoA/anammox* and *nosZ*/bacteria (Table 4). A greater direct contribution of *nosZ*/bacteria (90.0%) to TN reduction compared with *amoA/anammox* (-1.0%) was observed in P₂ over the entire period (Figure 4b). The *amoA/anammox* variable was negatively linked with the NO_2^- -N accumulation rates, while the variable *nosZ*/bacteria were positively linked with the TN reduction rate. The *nosZ* gene is currently accepted as a representative for the complete degree of the denitrification process [39,57]. Thus, an increasing *nosZ* represents the level of TN transformation. The variable *anammox/amoA*, which is identified as NO_2^- -N consumption, exhibits a positive link with the NH_4^+ -N and NO_3^- -N transformations in P₂ because *anammox* is responsible for NO_2^- -N consumption, whereas *amoA* is responsible for NO_2^- -N accumulation. Thus, the consumption ratio suggests the extent or level of NH_4^+ -N transformation. More NO_2^- -N consumption results in a higher NH_4^+ -N transformation. The *nrxA*/bacteria variable exhibits a positive link with the NH_4^+ -N transformation rate. The *nrxA* gene directly consumes NO_2^- -N and, thus, the consumption ratio indirectly represents the transformation of NH_4^+ -N. The above results indicate that combined *anammox*/nitrification (i.e. completely autotrophic nitrogen removal over nitrite; CANON) was contributed to NH_4^+ -N and TN removal [36,54].

The results from Figure 4c indicated that *anammox/amoA* was the key factor contributing to the high reduction of NH_4^+ -N (95.6%) in P₃. A higher direct effect of $(\text{napA} + \text{narG})/\text{nrxA}$ (53.3%) on the NO_3^- -N reduction compared with *anammox/amoA* (46.6%) was observed in P₃ (Figure S3c). The TN reduction rate in P₃ was significantly correlated with the ratios of $(\text{napA} + \text{narG} + \text{nirK} + \text{nirS} + \text{nosZ})/\text{bacteria}$ and *anammox*/bacteria. A higher direct effect of *anammox*/bacteria (49.2%) on TN reduction compared with $(\text{napA} + \text{narG} + \text{nirK} + \text{nirS} + \text{nosZ})/\text{bacteria}$ (39.6%) was observed in P₃ (Figure 4c). The two variables were directly involved in the consumption of NH_4^+ -N and NO_3^- -N during the *anammox* and denitrification processes and were, therefore, positively linked with the TN reduction. Thus, both *anammox* and denitrified microorganisms contributed to the TN reduction. On the functional gene level, the results suggest that the co-occurrence of simultaneous nitrification, *anammox*, and denitrification (SNAD) processes can be conducive for the simultaneous and enhanced removal of N and COD in the biofilter system [22,58,59].

Environmental Implications

Biofilter systems have been largely explored and adopted as a well-known technology to remove carbon and nitrogen contaminants from wastewater. Our results indicate that the high removal potential and adaptability to remove COD, NH_4^+ -N and TN from domestic wastewater were observed in a single vertical-flow biofilter. The maximum pollutant concentrations (COD=32.76 mg/L, NH_4^+ -N=2.63 mg/L and TN=6.79 mg/L) in the effluent from the biofilter were lower than the most rigorously regulated Class 1 A values (COD \leq 50 mg/L, TN \leq 15 mg/L, and NH_4^+ -N \leq 5 mg/L) in the China National Standard (GB18918-2002).

To protect the surface water environment, many developing countries have established stricter statutes and restrictive standards to limit the total emission of TN [60]. Therefore, the comprehensive advantages of technical feasibility and easy operation (without the requirements of continuous aeration operations or extra running costs) offer principal benefits for the utilization of a biofilter as an advanced treatment technique to promote TN removal from domestic wastewater, especially in rural areas of developing countries. This study suggests great potential for the real application of a vertical-flow biofilter for treating domestic wastewater. It may become a sustainable and affordable domestic wastewater purification method in remote or economically depressed regions of developing countries. However, the engineering applications of biofilter systems still need further study.

CONCLUSION

In this study, a three-stage vertical flow biofilter without extra aeration running achieved high removal efficiencies of TN ($87.00 \pm 2.59\%$, $33.69 \pm 7.93 \text{ g m}^{-2} \text{ d}^{-1}$), NH_4^+ -N ($95.90 \pm 2.44\%$, $24.17 \pm 6.23 \text{ g m}^{-2} \text{ d}^{-1}$), and COD ($92.00 \pm 3.07\%$, $558.15 \pm 208.47 \text{ g m}^{-2} \text{ d}^{-1}$). NH_4^+ -N and TN removal contributions can be ranked as follows: P₁ (45.9% and 38.4% respectively) > P₂ (39.6% and 28.2% respectively) > P₃ (10.6% and 20.5% respectively). Specifically, NO_3^- -N removal rates in P₃ was notably enhanced, resulting in apparent decline of NO_3^- -N and TN in the effluent. The coupling of nitrification and denitrification was contributed to the robust NH_4^+ -N and TN removal in P₁. The combined *anammox* and nitrification was contributed to NH_4^+ -N and TN removal in P₂. The combined *anammox* and denitrification accounted for the robust TN reduction in P₃.

ACKNOWLEDGMENTS

This work was supported by the science and technology project of the Yangling Demonstration Zone (2016SF-05), Fundamental Research Funds for Central Universities (Z109021711), and the Start-up Funds of Northwest A & F University (for Honglei Wang; Z109021610).

REFERENCES

1. Ryu HD and Lee SI. Comparison of 4-stage biological aerated filter (BAF) with MLE process in nitrogen removal from low carbon-to-nitrogen wastewater. *Environ Eng Sci*. 2009;26:163-170.
2. Pujol R, et al. Biofilters: flexible, reliable biological reactors. *Wat Sci Tech*. 1994;29:33-38.
3. Zeng TT, et al. Nitrogen removal efficiency and microbial community analysis of ANAMMOX biofilter at ambient temperature. *Water Sci Technol*. 2015;71:725-733.
4. Chatterjee P, et al. Development of anammox process for removal of nitrogen from wastewater in a novel self-sustainable biofilm reactor. *Bioresour Technol*. 2016;218:723-730.
5. Zhang Y, et al. Performance of system consisting of vertical flow trickling filter and horizontal flow multi-soil-layering reactor for treatment of rural wastewater. *Bioresour Technol*. 2015a;193:424-432.
6. Ji G, et al. Association of nitrogen micro-cycle functional genes in subsurface wastewater infiltration systems. *Ecol Eng*. 2012;44:269-277.
7. Yang N, et al. Performance and microbial community of a novel non-aeration-based up-flow bioelectrochemical filter (UBEF) treating real domestic wastewater. *Chem Eng J*. 2018;348:271-280.
8. Wang H, et al. Review on the Fate and Mechanism of Nitrogen Pollutant Removal from Wastewater Using a Biological Filter. *Pol. J Environ Stud*. 2017;26.
9. Wik T. Trickling filters and biofilm reactor modelling. *Rev Environ Sci Bio*. 2003;2:193-212.
10. Ruan YJ, et al. Bacterial Community Analysis of Different Sections of a Biofilter in a Full-Scale Marine Recirculating Aquaculture System. *N Am J Aquacult*. 2015;77:318-326.
11. Rocher V, et al. Nitrite accumulation during denitrification depends on the carbon quality and quantity in wastewater treatment with biofilters. *Environ Sci Pollut Res*. 2015;22:10179-10188.
12. Mulder J, et al. Full-scale application of the SHARON process for treatment of rejection water of digested sludge dewatering. *Water Sci Technol*. 2001;43:127-134.
13. Bernet N, et al. Nitrification at low oxygen concentration in biofilm reactor. *J Environ Eng*. 2001;127:266-271.
14. Zhang Y, et al. Functional gene groups controlling nitrogen transformation rates in a groundwater-restoring denitrification biofilter under hydraulic retention time constraints. *Ecol Eng*. 2016b;87:45-52.
15. Blázquez E, et al. Performance, limitations and microbial diversity of a biotrickling filter for the treatment of high loads of ammonia. *Chem Eng J*. 2017;311:91-99.
16. Zhang Y, et al. Drivers of nitrous oxide accumulation in denitrification biofilters with low carbon: nitrogen ratios. *Water Res*. 2016a;106:79-85.
17. Guillón JS, et al. Autotrophic nitrogen removal over nitrite in a sponge-bed trickling filter. *Bioresour Technol*. 2015;187:314-325.
18. Tsang YF, et al. Effects of high ammonia loads on nitrogen mass balance and treatment performance of a biotrickling filter. *Process Saf Environ*. 2015;98:253-260.
19. Van Den Akker B, et al. Application of high rate nitrifying trickling filters for potable water treatment. *Water Res*. 2008;42:4514-4524.
20. Ji G, et al. The spatial distribution of nitrogen removal functional genes in multimedia biofilters for sewage treatment. *Ecol Eng*. 2013;55:35-42.
21. Zhang Y, et al. Genetic associations as indices of nitrogen cycling rates in an aerobic denitrification biofilter used for groundwater remediation. *Bioresour Technol*. 2015b;194:49-56.
22. Zhi W, et al. Enhanced long-term nitrogen removal and its quantitative molecular mechanism in tidal flow constructed wetlands. *Environ Sci Technol*. 2015;49:4575-4583.

23. Pang Y, et al. Cold temperature effects on long-term nitrogen transformation pathway in a tidal flow constructed wetland. *Environ Sci Technol.* 2015;49:13550-13557.
24. Apha. Standard methods for the examination of water and wastewater american public health association. Washington DC. 1995.
25. Mulder A, et al. Anaerobic ammonium oxidation discovered in a denitrifying fluidized bed reactor. *FEMS Microbiol Ecol.* 1995;16:177-183.
26. Dionisi HM, et al. Quantification of nitrosomonas oligotropha-like ammonia-oxidizing bacteria and nitrospira spp. from full-scale wastewater treatment plants by competitive PCR. *Appl Environ Microb.* 2002;68:245-253.
27. Fierer N, et al. Assessment of soil microbial community structure by use of taxon-specific quantitative PCR assays. *Appl Environ Microb.* 2005;71:4117-4120.
28. Großkopf R, et al. Diversity and structure of the methanogenic community in anoxic rice paddy soil microcosms as examined by cultivation and direct 16S rRNA gene sequence retrieval. *Appl Environ Microb.* 1998;64:960-969.
29. Tsushima I, et al. Quantification of anaerobic ammonium-oxidizing bacteria in enrichment cultures by real-time PCR. *Water Res.* 2007;41:785-794.
30. Poly F, et al. First exploration of Nitrobacter diversity in soils by a PCR cloning-sequencing approach targeting functional gene nxrA. *Fems Microbiol Lett.* 2008;63:132-140.
31. Bru D, et al. Relative Abundances of Proteobacterial Membrane-Bound and Periplasmic Nitrate Reductases in Selected Environments. *Appl Environ Microb.* 2007;73:5971-5974.
32. Lpez-Gutiérrez JC, et al. Quantification of a novel group of nitrate-reducing bacteria in the environment by real-time PCR. *J Microbiol Meth.* 2004;57:399-407.
33. Yan TF, et al. Molecular diversity and characterization of nitrite reductase gene fragments (nirK and nirS) from nitrate- and uranium-contaminated groundwater. *Environ Microbiol.* 2003;5:13-24.
34. Scala DJ and Kerkhof LJ. Nitrous oxide reductase (nosZ) gene-specific PCR primers for detection of denitrifiers and three nosZ genes from marine sediments. *Fems Microbiol Lett.* 1998;162:61-68.
35. Zhi W and Ji G. Quantitative response relationships between nitrogen transformation rates and nitrogen functional genes in a tidal flow constructed wetland under C/N ratio constraints. *Water Res.* 2014;64:32-41.
36. Liang Y, et al. Performance and influence factors of completely autotrophic nitrogen removal over nitrite (CANON) process in a biofilter packed with volcanic rocks. *Environ Technol.* 2015;36:946-952.
37. Latrach L, et al. Domestic wastewater disinfection by combined treatment using multi-soil-layering system and sand filters (MSL-SF): A laboratory pilot study. *Ecol Eng.* 2016;91:294-301.
38. Latrach L, et al. Two-stage vertical flow multi-soil-layering (MSL) technology for efficient removal of coliforms and human pathogens from domestic wastewater in rural areas under arid climate. *Int J Hyg Envir Heal.* 2018;221:64-80.
39. Canfield DE, Glazer AN, Falkowski PG 2010 The evolution and future of Earth's nitrogen cycle. *Science.* 330 192-196.
40. Cui B, et al. Achieving partial denitrification through control of biofilm structure during biofilm growth in denitrifying biofilter. *Bioresour Technol.* 2017;238:223-231.
41. Ji B, et al. Domestic wastewater treatment in a novel sequencing batch biofilm filter. *Appl Microbiol Biot.* 2015;99:5731-5738.
42. Lan CJ, et al. Development of simultaneous partial nitrification, anammox and denitrification (SNAD) process in a sequential batch reactor. *Bioresour Technol.* 2011;102:5514-5519.
43. Kim S, et al. Evaluation of denitrification-nitrification biofilter systems in treating wastewater with low carbon: nitrogen ratios. *Environ Technol.* 2015;36:1035-1043.
44. Jing ZQ, et al. Practice of integrated system of biofilter and constructed wetland in highly polluted surface water treatment. *Ecol Eng.* 2015b;75:462-469.
45. Gao Y, et al. High performance of nitrogen and phosphorus removal in an electrolysis-integrated biofilter. *Water Sci Technol.* 2016;74:714-721.
46. Schleper C. Ammonia oxidation: different niches for bacteria and archaea? *ISME J.* 2010;4:1092-1094.

47. Prosser JI and Nicol GW. Archaeal and bacterial ammonia-oxidisers in soil: the quest for niche specialisation and differentiation. *Trends Microbiol.* 2012;20:523-531.
48. Daverey A, et al. Effect of zinc on anammox activity and performance of simultaneous partial nitrification, anammox and denitrification (SNAD) process. *Bioresour Technol.* 2014;165:105-110.
49. Kandeler E, et al. Abundance of narG, nirS, nirK, and nosZ genes of denitrifying bacteria during primary successions of a glacier foreland. *Appl Environ Microb.* 2006;72:5957-5962.
50. Hallin S, et al. Metabolic Profiles and Genetic Diversity of Denitrifying Communities in Activated Sludge after Addition of Methanol or Ethanol. *Appl Environ Microb.* 2006;72:5445-5452.
51. De Sanctis M, et al. Integration of an innovative biological treatment with physical or chemical disinfection for wastewater reuse. *Sci Total Environ.* 2016;543:206-213.
52. Hwang Y-W, et al. Simultaneous nitrification/denitrification in a single reactor using ciliated columns packed with granular sulfur. *Water Qual Res J Can.* 2005;40:91-96.
53. Jones CM, et al. Phylogenetic analysis of nitrite, nitric oxide, and nitrous oxide respiratory enzymes reveal a complex evolutionary history for denitrification. *Molecular biology and evolution.* 2008;25:1955-1966.
54. Liu T, et al. Biodiversity and quantification of functional bacteria in completely autotrophic nitrogen-removal over nitrite (CANON) process. *Bioresour Technol.* 2012;118:399-406.
55. Cua LS and Stein LY. Effects of nitrite on ammonia-oxidizing activity and gene regulation in three ammonia-oxidizing bacteria. *Fems Microbiol Lett.* 2011;319:169-175.
56. Jin R-C, et al. Performance and robustness of an ANAMMOX anaerobic baffled reactor subjected to transient shock loads. *Bioresour Technol.* 2012;114:126-136.
57. Stres B, et al. Nitrous oxide reductase (nosZ) gene fragments differ between native and cultivated michigan soils. *Appl Environ Microb.* 2004;70:301-309.
58. Jiang H, et al. A pilot-scale study on start-up and stable operation of mainstream partial nitrification-anammox biofilter process based on online pH-DO linkage control. *Chem Eng J.* 2018
59. Yu J-J and Jin RC. The ANAMMOX reactor under transient-state conditions: Process stability with fluctuations of the nitrogen concentration, inflow rate, pH and sodium chloride addition. *Bioresour Technol.* 2012;119:166-173.
60. Vçurçsmarty CJ, et al. Global threats to human water security and river biodiversity. *Nature.* 2010;467:555-561.